

The behaviour of trace elements in high-P mineral assemblages: a LA-ICP-MS study of mafic rocks from the Nevado-Filábride complex (SE Spain)

Autor(en): **Molina, José F. / Montero, Pilar**

Objektyp: **Article**

Zeitschrift: **Schweizerische mineralogische und petrographische Mitteilungen
= Bulletin suisse de minéralogie et pétrographie**

Band (Jahr): **83 (2003)**

Heft 1

PDF erstellt am: **06.08.2024**

Persistenter Link: <https://doi.org/10.5169/seals-63138>

Nutzungsbedingungen

Die ETH-Bibliothek ist Anbieterin der digitalisierten Zeitschriften. Sie besitzt keine Urheberrechte an den Inhalten der Zeitschriften. Die Rechte liegen in der Regel bei den Herausgebern.

Die auf der Plattform e-periodica veröffentlichten Dokumente stehen für nicht-kommerzielle Zwecke in Lehre und Forschung sowie für die private Nutzung frei zur Verfügung. Einzelne Dateien oder Ausdrucke aus diesem Angebot können zusammen mit diesen Nutzungsbedingungen und den korrekten Herkunftsbezeichnungen weitergegeben werden.

Das Veröffentlichen von Bildern in Print- und Online-Publikationen ist nur mit vorheriger Genehmigung der Rechteinhaber erlaubt. Die systematische Speicherung von Teilen des elektronischen Angebots auf anderen Servern bedarf ebenfalls des schriftlichen Einverständnisses der Rechteinhaber.

Haftungsausschluss

Alle Angaben erfolgen ohne Gewähr für Vollständigkeit oder Richtigkeit. Es wird keine Haftung übernommen für Schäden durch die Verwendung von Informationen aus diesem Online-Angebot oder durch das Fehlen von Informationen. Dies gilt auch für Inhalte Dritter, die über dieses Angebot zugänglich sind.

The behaviour of trace elements in high-P mineral assemblages: a LA-ICP-MS study of mafic rocks from the Nevado-Filábride complex (SE Spain)

José F. Molina¹ and Pilar Montero¹

Abstract

Trace-element data (obtained by LA-ICP-MS) from garnet, clinopyroxene, amphibole, zoisite/epidote, paragonite and phengite from foliated eclogites and coronitic metagabbros and high-pressure amphibolites from the Nevado-Filábride complex (SE Spain) are reported in this work. Rb, Cs and Ba are concentrated in white mica, whereas Y and HREE are in garnet, and Sr and LREE in epidote and zoisite. Even though whole-rock Σ REE can be up to ca. 100 ppm, amphibole and clinopyroxene show REE contents (Σ REE ca. 1–10 ppm) significantly lower than those of minerals with an igneous origin. Sr and LREE present large scattering at single-grain scale in minerals from eclogites. This contrasts with a more systematic trace-element distribution in high-P amphibolites.

Accordingly, electron microprobe analyses of epidote from foliated eclogites reveal the existence of micrometer-scale irregular patches with very high Sr and LREE contents (ca. 2000 ppm La, 6000 ppm Ce and > 4000 ppm Sr) related to rutile inclusions. The data suggest that titanite, which could be an early Sr-LREE-rich mineral, could cause local Sr and LREE release when transformed to rutile during the eclogite-facies metamorphism, leading to the heterogeneous distribution of these trace elements in the rock matrix. The preservation of these fine-scale compositional heterogeneities provides evidence for limited mass transport during the eclogite-facies metamorphism, which differs from equilibrium observed in high-P amphibolites. Different fluid-transport scales may account for such trace-element behaviour.

Keywords: eclogite-facies metamorphism, mafic rocks, mineral trace elements, LA-ICP-MS, Nevado-Filábride complex.

1. Introduction

Interest in understanding petrogenetic processes in the mantle and lower crust has led to a large number of studies on the trace-element distribution in minerals from high-grade crustal and mantle rocks (e.g. Rampone et al., 1993; Bea et al., 1994, 1998; Bea, 1996; Zanetti et al., 1996; Ionov et al., 1997). Though equally important, systematic trace-element studies on minerals from high-P, low-T rocks are much scarcer (e.g. Messiga et al., 1995; Tribuzio et al. 1996; Nagasaki and Enami, 1998; Zack et al., 2001; Hermann, 2002).

High-P experiments on H₂O- and CO₂-H₂O-bearing basalts (e.g. Schmidt and Poli, 1998; Molina and Poli, 2000; Poli and Schmidt, 2002), and geochemical characteristics of volcanic-arc rocks (e.g. Ryan et al. 1996; Elliot et al., 1997) suggest that fluids are released from the subducting slab causing progressive depletion in incompatible elements as devolatilisation reactions progress. These fluids modify the mantle source of island-arc basalts, which are characterised by relatively

low abundances of Nb and Ta relative to LREE and large ion lithophile elements (e.g. Saunders et al., 1980; Tatsumi and Eggins, 1993). Tribuzio et al. (1996) showed that garnet, allanite, epidote, lawsonite, titanite and apatite account for most of the REE budget of high-P, low-T mafic rocks. The stability of lawsonite and epidote up to ultrahigh-P conditions (Poli and Schmidt, 1995, 1998) suggests that these mineral phases are relevant for REE recycling at convergent margins. However, in spite of their potential importance, these mineral phases are not taken into account in estimates of the trace-element composition of fluids from subducting slabs (e.g. Brenan et al., 1995a, b; Keppler, 1996; Ayers et al., 1997). To obtain more realistic models of trace element and in particular REE recycling at convergent margins a better understanding of trace-element distribution among eclogite-facies minerals is necessary.

On the other hand, fluid behaviour in high-P rocks is not yet well constrained. Large scale-fluid flow is required for the eclogitisation of subducted dry crust (Austrheim et al., 1997) and for meta-

¹ Departamento de Mineralogía y Petrología, Campus de Fuentenueva, University of Granada, 18002-Granada, Spain. <jfmolina@ugr.es>

somatism in paleo-subduction zones (e.g. Sorensen and Grossman, 1989; Bebout and Barton, 1993). However, fine-scale chemical and isotopic heterogeneities reported in eclogite-facies rocks rather suggest local fluid flow (e.g. Selverstone et al., 1992; Getty and Selverstone, 1994; Scambelluri and Philippot, 2001). Trace elements are more sensitive to time-dependent processes than major elements (e.g. Hickmott et al., 1987; Hickmott and Shimizu, 1990). In addition, they are very sensitive to fluid-rock interaction processes and, hence, can give constraints about the scale of fluid flow during high-P metamorphism (e.g. Hickmott et al., 1987; Getty and Selverstone, 1994).

Coronitic metagabbros and texturally equilibrated foliated eclogites and high-P amphibolites crop out in the Nevado-Filábride complex (Betic Cordilleras, SE Spain). Metagabbros may present relict igneous mineralogy. When eclogitisation of these rock types runs to completion, hydrous phases such as amphibole and zoisite/clinozoisite are abundant, providing evidence for the importance of fluids in the gabbro-eclogite transition. High-P amphibolites exhibit epidote segregation

at centimetre-to-metre scale, which was, probably, fluid controlled. Therefore, a systematic study of trace elements in high-P minerals from these rock types can give insights into how fluids and deformation influence the distribution of trace elements at high-P conditions.

In this paper, we report the results of systematic trace-element analyses of amphibole, garnet, clinopyroxene, epidote-group minerals, and white mica from Nevado-Filábride mafic rocks, determined by laser ablation connected to an inductively-coupled mass spectrometer (LA-ICP-MS). The importance of epidote and its reactional history in the distribution of LREE and Sr at high-P conditions are also emphasised.

2. Geological setting and petrography

The Nevado-Filábride complex is an Alpine metamorphic terrain situated in the Betic Cordilleras (SE Spain, Fig. 1), which experienced high-P metamorphism with amphibolite-facies overprint (e.g. Gómez-Pugnaire and Fernández-Soler, 1987; Molina and Poli, 1998).

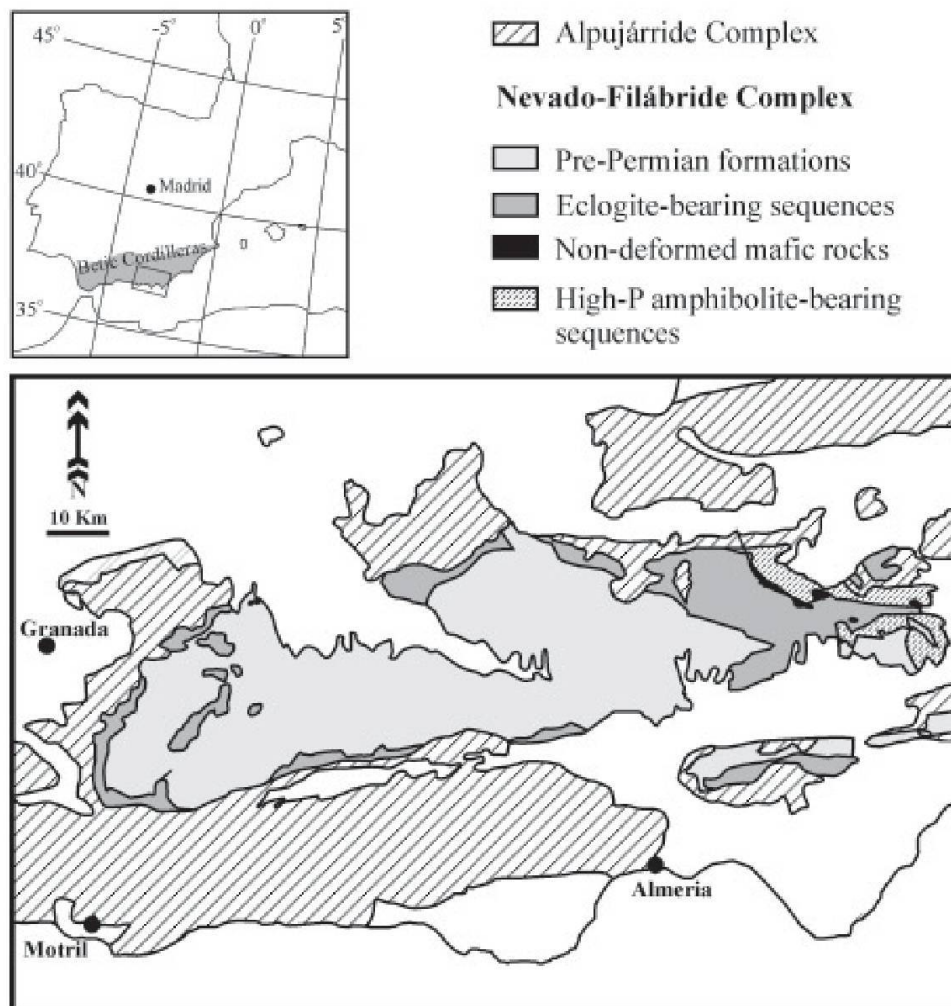


Fig. 1 Structural map of the Nevado-Filábride complex showing the distribution of the mafic rocks.

Table 1 Mineral assemblages from the Nevado-Filábride complex analysed by LA-ICP-MS.

Rock type	Assemblage	Textural features	LA-ICP-MS analysed phases
Coronitic metagabbro	Gar, Cpx, Zo, Q, Ru	Decussate aggregates of Zo and Cpx. Coronas of Gar	Cpx, Gar, Zo
Foliated eclogite	Na-Ca Amp, Gar, Cpx, Pg, Ep, Q, Ru	Abundant Ep inclusions in Gar cores. Coronas of Ep, Ca Amp around Gar. Ab, Ca Amp in symplectites	Cpx, Gar, Amp, Ep, Pg
Paragonite-bearing high- <i>P</i> amphibolite	Na-Ca Amp, Gar, Pg, Q, Ru	Traces of Ep included in Gar. Ep absent in the rock matrix	Gar, Amp, Pg
Phengite-bearing high- <i>P</i> amphibolite	Na-Ca Amp, Gar, Pheng, Q, Ru	Ep inclusions in Gar cores. Ep absent in the rock matrix	Gar, Amp, Pheng

Mineral abbreviations: Ab—albite; Amp—amphibole; Ca Amp—calcic amphibole; Ep—epidote; Gar—garnet; Na-Ca Amp—sodic-calcic amphibole; Pg—paragonite; Pheng—phengite; Cpx—clinopyroxene; Q—quartz; Ru—rutile; Zo—zoisite.

This metamorphic complex contains a Permo-Triassic or younger sequence with metapsammities and grey schists with relatively large blocks of metadolerites and metagabbros at the base, and marbles and calc-schists with intercalations of small bodies of amphibolites and serpentinites at the top (García-Dueñas et al., 1992; Jabaloy et al., 1993). The mafic rocks formed during late Jurassic alkaline to transitional continental magmatism (e.g. Gómez-Pugnaire et al., 2000).

Based on textural features and high-*P* mineral assemblages, three types of metabasites can be distinguished in the Nevado-Filábride complex (Table 1) (see Gómez-Pugnaire and Fernández-Soler (1987) and Molina and Poli (1998) for details):

1) Coronitic metagabbros: undeformed, coarse-grained metagabbros with aggregates of omphacite + sodic-calcic amphibole ± rutile (grain size ~100–200 µm) replacing igneous clinopyroxene, sodic-calcic amphibole after olivine, zoisite after plagioclase, and garnet coronas around omphacite and zoisite aggregates.

2) Foliated eclogites: sheared mafic rocks with a foliation defined by compositional banding of millimetre-scale paragonite, and sodic-calcic amphibole + omphacite ± epidote ± rutile layers with grain sizes ranging from 100 to 200 µm. Idiomorphic porphyroblasts of garnet ($\varnothing = 1\text{--}2$ mm) are also present, with cores extremely rich in randomly distributed inclusions of amphibole, epidote, quartz and rutile, and inclusion-free rims.

3) High-*P* amphibolites: sheared mafic rocks with a coarse foliation (grain size 0.5 to 1 mm) defined by abundant sodic-calcic amphibole,

white mica (paragonite or phengite), rutile and/or titanite. In addition, pure albite can be present in paragonite-bearing assemblages. Epidote is very rare in the rock matrix, occurring mostly as inclusions in garnet. As in the foliated eclogites, garnet shows cores with inclusions of amphibole, epidote and quartz and inclusion-free rims.

In addition, rare zircon and apatite, very rare zirconolite and baddeleyite included in rutile may also be present in the three rock types.

In the western sector of the Nevado-Filábride complex (Fig. 1), well-exposed foliated eclogites occur as metre-thick parallel bands intercalated between metapsammities and graphitic mica-schists. In addition, there are large bodies (up to 50 m thick) of coronitic metagabbros, locally crosscut by high-*P* veins filled with abundant quartz and kyanite and moderate to scarce paragonite, zoisite and omphacite.

In the eastern sector, high-*P* amphibolites occur as metre to tens of metre-thick sheared layers in the upper metacarbonate sequences. It is important to note that epidote is very rare in the rock matrix of these amphibolites, being concentrated in centimetre-scale boudins and in centimetre-scale thick layers. This suggests the segregation of epidote at centimetre- to metre-scales, with important implications on the redistribution of Sr and LREE during metamorphism as discussed later.

The lower metapelite sequences in the eastern sector of the Nevado-Filábride complex contain large blocks of eclogites, commonly with preserved igneous mineralogy comprising gabbros,

dolerites and basaltic dykes. Extremely peraluminous xenoliths occur locally in gabbros and dolerites providing evidence for continental magmatism (e.g. Gómez-Pugnaire and Muñoz, 1991).

Table 2 Whole-rock analyses (major and trace elements in wt% and ppm, respectively).

	1a	1b	2	3	4a	4b
SiO ₂	45.4	45.9	49.9	47.1	49.9	48.5
TiO ₂	1.13	2.20	1.24	0.75	1.35	2.17
Al ₂ O ₃	16.4	14.9	15.2	17.5	16.7	14.9
Fe ₂ O ₃	18.2	13.9	8.99	8.56	9.87	12.2
MgO	7.16	8.82	8.95	11.1	6.79	6.42
MnO	0.17	0.21	0.15	0.15	0.16	0.22
CaO	5.98	7.84	8.84	9.67	9.05	7.92
Na ₂ O	3.98	3.17	4.60	3.18	4.24	3.71
K ₂ O	0.25	0.94	0.19	0.21	0.44	0.79
P ₂ O ₅	0.18	0.38	0.21	0.09	0.18	0.32
LOI	1.16	1.51	1.63	1.33	1.32	0.92
Total	100	100	99.9	99.7	100	98.2
Mg#	0.48	0.59	0.69	0.75	0.61	0.54
Ne	1.28	0.48	2.58	2.13	0.91	—
Hy	—	—	—	—	—	2.45
Ol	15.8	12.1	8.26	12.4	7.20	5.78
Li	15.1	42.7	19.1	6.57	25.5	44.6
Rb	1.40	18.6	—	—	7.27	13.9
Cs	0.13	1.11	—	—	0.63	0.83
Sr	123	93.0	352	238	360	280
Ba	12.9	36.4	—	685	44.4	94.4
Sc	60.1	59.9	39.1	18.7	60.9	36.8
V	208	324	221	115	263	202
Co	24.6	35.8	70.1	71.7	26.0	67.7
Zr	79.0	246	125	43.7	99.0	115
Y	23.9	41.1	28.1	11.4	19.5	30.3
Nb	3.23	8.82	1.26	1.21	6.75	17.0
Ta	0.52	1.18	—	—	0.87	2.54
Th	0.33	0.66	2.08	1.72	0.53	1.25
U	0.49	0.25	0.21	0.01	0.13	0.26
La	4.28	9.23	8.92	3.56	7.23	15.5
Ce	10.0	27.3	20.9	8.58	17.2	36.2
Pr	1.54	4.05	3.11	1.15	2.51	5.00
Nd	7.37	19.6	14.4	4.79	11.9	23.4
Sm	2.29	5.74	4.38	1.70	3.27	6.37
Eu	0.99	1.69	1.74	0.78	1.33	2.10
Gd	2.82	5.74	5.11	2.21	3.62	7.67
Tb	0.60	1.08	0.81	0.34	0.60	1.12
Dy	3.82	6.86	5.07	2.05	3.59	6.22
Ho	0.90	1.58	1.02	0.44	0.74	1.19
Er	2.43	4.31	2.62	1.10	1.91	3.22
Tm	0.40	0.75	0.39	0.15	0.28	0.42
Yb	2.24	4.31	2.50	0.90	1.59	2.49
Lu	0.34	0.63	0.35	0.14	0.23	0.36
ΣREE	40.0	92.9	71.3	27.9	56.0	111
Eu/Eu*	1.19	0.90	1.13	1.23	1.18	0.92
La _N /Lu _N	1.35	1.56	2.70	2.69	3.37	4.60

1, high-P amphibolite (a, paragonite-bearing type; b, phengite-bearing type); 2, foliated eclogite; 3, coronitic metagabbro; 4, igneous relic-bearing mafic rocks (a, metadolerite; b, metabasaltic dyke).

Thermobarometric estimates performed on garnet-omphacite and garnet-amphibole-albite-paragonite assemblages suggest formation of the high-P amphibolites at 500–550 °C and 9–12 kbar, and foliated and coronitic metagabbros at 500–600 °C and 12–25 kbar (Molina, 1995; Molina and Poli, 1998). The temperature and pressure estimates in high-P amphibolites are consistent with those reported by López-Sánchez-Vizcaíno et al. (1997) based on mineral equilibrium calculations for the associated carbonate rocks and also with minimum pressures of ca. 8 kbar for the occurrence of garnet in mafic systems at medium to low temperature conditions (Poli, 1993).

3. Analytical methods

3.1. Whole-rock analyses

Six samples representative of each lithotype studied in the Nevado-Filábride complex were collected for whole-rock analyses. Powders were obtained by crushing the rocks to a grain size of less than 5 millimetres in a crusher with hardened steel jaws and then grinding them in a tungsten carbide jar to a grain size of < 25 µm. This procedure produced no detectable contamination of REE or HFSE.

Major-element determinations were performed by XRF with a Philips PW 1404/10 spectrometer after fusion with lithium tetraborate (Centro de Instrumentación Científica (C.I.C.), University of Granada). Typical precision was better than ± 1.5 % relative for an analyte concentration of 10 wt%.

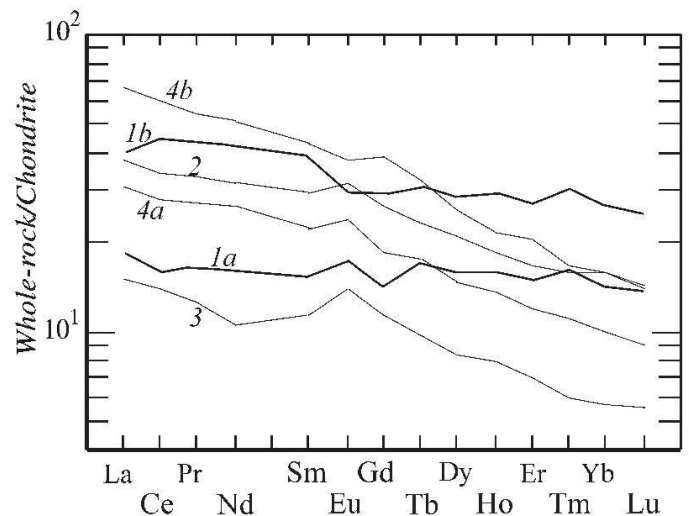


Fig. 2 Chondrite-normalized REE patterns of whole-rock samples. 1a, high-P amphibolite (paragonite-rich type); 1b, high-P amphibolite, (phengite-rich type); 2, foliated eclogite; 3, coronitic metagabbro; 4a, metadolerite; 4b, metabasalt. See Table 2 for whole-rock analyses. Chondrite values are from Anders and Ebihara (1982).

Zircon was determined by XRF on pressed pellets, with a precision better than $\pm 4\%$ for 100 ppm Zr. Other trace-element determinations were carried out by ICP-Mass Spectrometry (ICP-MS) after $\text{HNO}_3 + \text{HF}$ digestion of 0.1000 g of sample powder in a Teflon-lined vessel at high *T* and *P*, evaporation to dryness, and subsequent dissolution in 100 ml of 4 vol% HNO_3 . Instrument measurements were performed in a PE SCIEX ELAN-5000 spectrometer using Rh as internal standard. Precision was about $\pm 2\%$ and $\pm 5\%$ rel for analyte concentrations of 50 and 5 ppm respectively.

3.2. Electron microprobe mineral analyses

Accessory minerals were identified using a Scanning Electron Microscope (SEM), operated in BSE and EDAX microanalysis, on a Zeiss DSM-950 microscope set at 20 kV. Major-element analyses of minerals were obtained by wavelength dispersion with a CAMECA Camebax SX-50 electron microprobe using natural and synthetic standards. Accelerating voltage was 20 kV and beam current was 15 nA. Precision was about ± 1.5 rel % for 1 wt% of analyte. Both procedures were performed at the University of Granada (C.I.C.).

Major elements, Sr, La and Ce in epidote were also analysed using a Cameca Camebax electron microprobe at the Mineralogical-Geological Museum (University of Oslo), using 15 kV acceleration voltage and 20 nA beam current.

3.3. LA-ICP-MS mineral analyses

Six metabasites (Table 1) covering the range of rock types studied in the present work were selected to determine the distribution of trace elements in high-*P* minerals.

The trace elements of individual mineral grains in thin sections (thickness ~ 80 μm) were analysed by LA ICP-MS in the Perkin Elmer Applications Laboratory at Überlingen (Germany) using an excimer UV laser ablation system coupled to a Perkin-Elmer Sciex Elan-6000 spectrometer (methods in Bea et al., 1996). The diameter of the laser beam was fixed to produce craters approximately 30 μm in diameter and 40–60 μm in depth. NBS-612 glass was used as an external standard for calibration. Concentration values were corrected using silicon as an internal standard, previously determined in every mineral by electron microprobe. Coefficients of variation (CV = $100 \times \text{SD}/\text{mean}$), obtained by measuring five replicates on a single grain of astrophyllite, were ± 4.2 rel % for 45.6 ppm La, ± 18.9 rel % for 0.57 ppm

Y, ± 4.4 rel % for 4.71 ppm Eu, and ± 11.3 rel % for 0.62 ppm Yb. For elements with concentrations higher than 100 ppm, CV are ± 1 – 3 rel % (see Bea et al., 1996). Under these conditions, detection limits were better than 20 ppb for most elements.

4. Whole-rock composition

Representative whole-rock analyses of the rock-types studied by LA-ICP-MS are given in Table 2. Data for non-deformed intrusive rocks with relics of kaersutite from the eastern sector of the Nevado-Filábride complex are shown for comparison.

The mafic rocks are compositionally comparable to alkaline-to-transitional basalts in that they are Hy-Ol-normative (Hy ~ 2.5) or Ne-normative (Ne = 0.48–2.58) with $\text{SiO}_2 = 45.4$ – 49.9 wt% and $\text{Na}_2\text{O} = 3.17$ – 4.60 wt%, although K_2O can be very low (0.19–0.94 wt%). CaO is variable, ranging from 5.98 wt% in high-*P* amphibolites to 9.67 wt% in coronitic metagabbros. Mg# values range from 0.48–0.59 in high-*P* amphibolites to 0.75 in the coronitic metagabbros. Mg# values are also high (~ 0.60) in metadolerite, but lower in the metabasalt, suggesting a higher degree of differentiation.

Alkaline trace elements are variable, with the highest values in the basaltic dyke (Table 2). Li, Rb and Cs contents in high-*P* amphibolites are higher than those in the coronitic gabbros and foliated eclogites, in which Rb and Cs are below detection limit (ca. 0.01 ppm). It is interesting to note that in epidote-free, high-*P* amphibolites, Sr contents are relatively low (~ 90 – 125 ppm), whereas in the other rock types these are significantly higher (>230 ppm). In the analysed rocks, V is relatively high (~ 100 – 325 ppm), while Sc and Y are moderate (~ 10 – 60 ppm). Zr is also relatively high (79–246 ppm), although in coronitic metagabbros it is moderate (~ 44 ppm). Ba contents are very variable, reaching 685 ppm in the coronitic metagabbros, whereas in the foliated eclogites they are below detection limit. Nb contents are relatively low (~ 5 – 9 ppm in high-*P* amphibolites and < 2 ppm in eclogites), although in the metabasalt they reach 17 ppm. Th and U contents are very low, with Th generally 2–10 times more abundant than U. REE contents are low or moderate in high-*P* amphibolites and coronitic metagabbros ($\Sigma\text{REE} \sim 40$ and 28 ppm, respectively), and high in the metabasalt ($\Sigma\text{REE} \sim 110$ ppm).

The chondrite-normalized REE patterns (Fig. 2) for the high-*P* amphibolites are almost flat ($\text{La}_N/\text{Lu}_N \sim 1.40$) with a negligible or no Eu anomaly, similar to those shown by E-MORB. Howev-

Table 3 Major-element mineral analyses (results in wt%).

	Amp 1r	Amp 1c	Amp 2r	Amp 2c	Ep 1i	Ep 2r	Ep 2c	Ep 3	Gar 1r	Gar 1c	Gar 2r	Gar 2c	Gar 3r	Gar 3c	Cpx 2	Cpx 3	Pheng 1	Pg 2
SiO ₂	46.05	46.53	43.66	47.67	36.45	37.13	38.21	38.92	37.9	37.76	38.45	37.93	38.89	38.76	55.27	56.31	47.22	46.72
TiO ₂	0.48	0.51	0.46	0.36	0.07	0.10	0.07	0.09	—	—	—	—	0.07	0.07	0.08	0.05	0.43	0.05
Al ₂ O ₃	12.88	12.72	12.85	12.55	23.36	25.42	26.98	30.25	21.12	20.93	21.33	20.24	21.76	21.29	9.62	12.14	30.61	38.72
Fe ₂ O ₃	—	—	—	—	13.93	9.82	8.74	4.28	—	—	—	—	—	—	—	—	—	—
FeO	15.59	14.87	14.11	10.81	—	—	—	—	30.16	30.96	24.75	29.7	29.23	28.79	7.39	4.83	2.94	0.85
MnO	—	—	0.13	0.06	0.22	0.13	0.17	0.08	0.82	1.45	1.48	2.17	0.36	1.18	0.03	0.02	—	—
MgO	9.87	9.89	11.57	12.1	0.04	0.01	0.05	—	2.56	2.17	3.29	3.33	2.99	1.15	7.53	7.5	2.09	0.14
CaO	8.69	7.72	9.68	7.18	22.7	23.17	23.00	24.92	8.41	7.56	11.56	7.53	8.92	11.15	12.73	11.74	0.01	0.21
Na ₂ O	2.98	3.9	3.79	4.62	—	—	—	—	—	—	—	—	—	—	7.15	7.39	1.11	7.18
K ₂ O	0.39	0.42	0.41	0.33	—	—	—	—	—	—	—	—	—	—	—	—	9.20	0.82
Total	96.93	96.56	96.66	95.68	96.77	95.78	97.22	98.54	100.97	100.83	100.9	100.9	102.22	102.39	99.8	99.98	93.61	94.69

1—high-P amphibolite; 2—foliated eclogite; 3—coronitic metagabbro; c—core; r—rim; i—inclusion in garnet.

er, in the other rock types, the chondrite-normalized REE patterns can show relatively high positive Eu anomalies ($\text{Eu}/\text{Eu}^* = 0.92\text{--}1.23$) and higher REE fractionation ($\text{La}_N/\text{Lu}_N \sim 2.70\text{--}4.60$). The variations in the REE fractionation may suggest that protoliths for high-P amphibolites and eclogites were derived from different magmatic sources. However, given the high contents of LREE in epidote (shown below), the segregation of epidote observed in high-P amphibolites strongly supports a relatively higher mobility of LREE during metamorphism.

5. Composition of major mineral phases

5.1. Amphibole

Amphibole in the eclogites and high-P amphibolites is mainly barrosite (see Table 3). NaM4-site occupancy is nearly identical in the two rock types (0.68–1.00 apfu), but eclogites show a higher A-site occupancy. During the low-P overprinting, these amphiboles are replaced by pargasite and hastingsite in the eclogites, and by actinolite or Mg-hornblende in the high-P amphibolites.

Amphibole contains low Rb, Cs and Y (0.02–8 ppm), moderate to high Li, Sc, Co and Zr (~1–100 ppm), and high V (~100–400 ppm) (see Table 4 and Fig. 3a). The REE contents of Nevado-Filábride amphiboles are extremely low when compared with amphiboles from igneous rocks (Fig. 4). ΣREE values in amphiboles from the Nevado-Filábride complex, for instance, are even lower than in ultramafic rocks, which show very low whole-rock REE contents. The low REE contents of Nevado-Filábride amphiboles are in agreement with values reported for Na-amphiboles from other high-P, low-temperature metamorphic belts (e.g. below detection limit of the ion microprobe in Na-amphiboles from Liguria; Tribuzio et al., 1996).

Most trace elements in amphibole with contents >1 ppm exhibit relatively minor variations at sample scale (e.g. $\sim 11.2 \pm 1.7$ ppm Sc, 129 ± 19 ppm V). However, Sr contents in amphibole from foliated eclogites are very variable ($\sim 400 \pm 350$ ppm). This contrasts with relatively minor scatter of Sr in amphibole from high-P amphibolites (16.2 ± 1.4 ppm), and may have important implications for the behaviour of trace elements at high-P conditions (see below).

There are significant differences in the distribution of REE among the Nevado-Filábride amphiboles. REE, particularly the LREE, are more abundant in amphibole from eclogite rocks (e.g. 0.17–2 ppm La in eclogitic amphibole and < 0.03

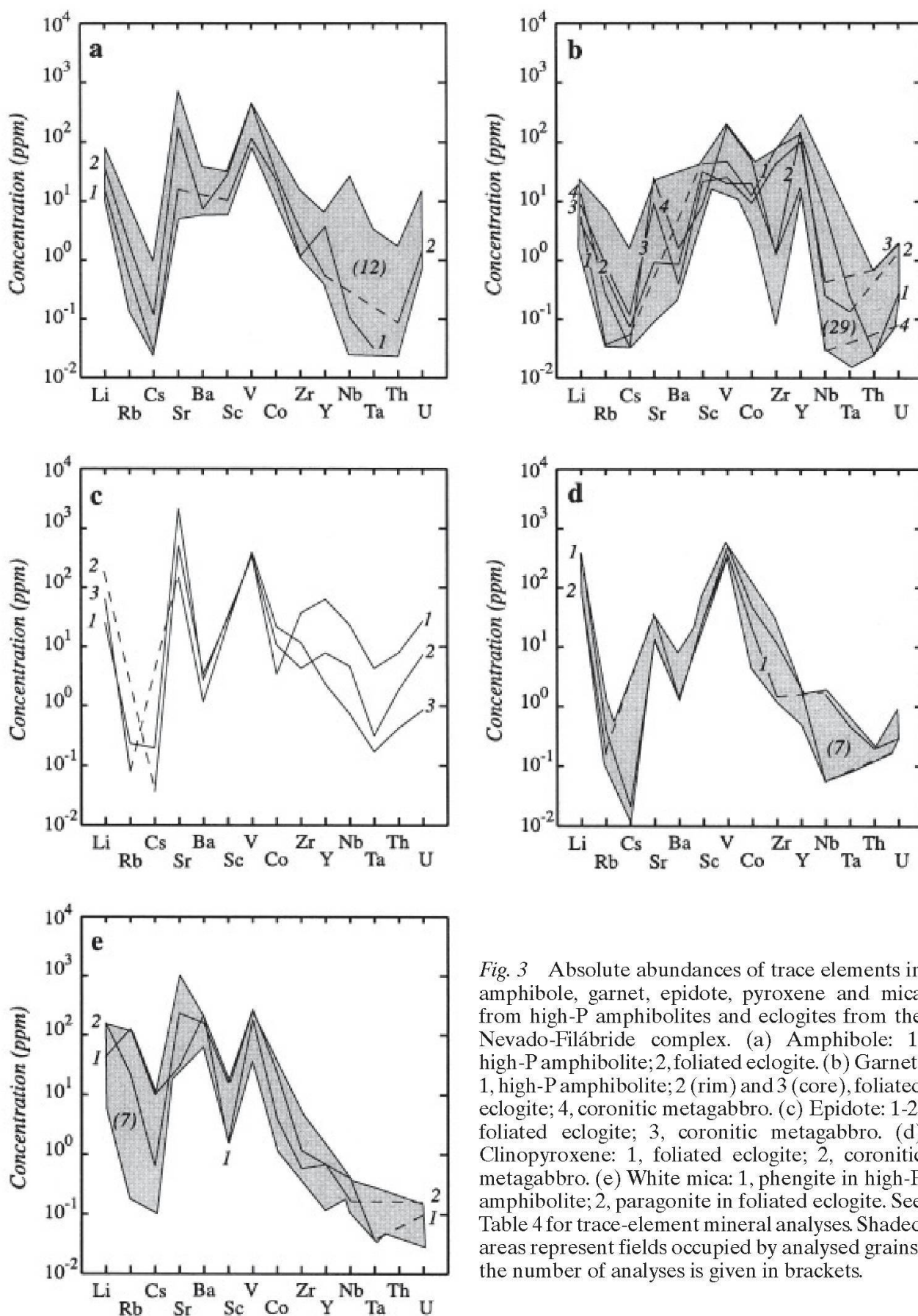


Fig. 3 Absolute abundances of trace elements in amphibole, garnet, epidote, pyroxene and mica from high-*P* amphibolites and eclogites from the Nevado-Filábride complex. (a) Amphibole: 1, high-*P* amphibolite; 2, foliated eclogite. (b) Garnet: 1, high-*P* amphibolite; 2 (rim) and 3 (core), foliated eclogite; 4, coronitic metagabbro. (c) Epidote: 1-2, foliated eclogite; 3, coronitic metagabbro. (d) Clinopyroxene: 1, foliated eclogite; 2, coronitic metagabbro. (e) White mica: 1, phengite in high-*P* amphibolite; 2, paragonite in foliated eclogite. See Table 4 for trace-element mineral analyses. Shaded areas represent fields occupied by analysed grains; the number of analyses is given in brackets.

ppm La in the amphibolites). Chondrite-normalized REE-patterns from eclogitic amphibole are almost flat or have slightly positive slopes with low fractionation of LREE/HREE ($La_N/Lu_N = 0.37-0.58$), whereas amphiboles from high-*P* am-

phibolites have clear positive slopes with $La_N/Lu_N = 0.02-0.05$ and no Eu anomaly (Fig. 5a). These contrasting patterns may be a consequence of the epidote segregation observed in high-*P* amphibolites as previously mentioned.

Table 4 Selected LA-ICP-MS analyses of major minerals from high-P amphibolites and eclogites (results in ppm).

	Amp 1	Amp 2	Amp 4	Amp 4	Ep 2	Ep 2	Ep 3	Gar 1	Gar 2r	Gar 2c	Gar 3	Cpx 2	Cpx 3	Pheng 1	Pg 2
Li	15.8	35.7	11.9	32.7	23.9	186	60.6	5.28	4.37	8.62	13.3	356	87.2	156	43.5
Rb	0.53	1.88	1.36	50.1	0.24	–	0.08	0.04	0.59	0.84	0.27	0.40	0.15	20.7	123
Cs	0.03	0.12	0.01	3.51	0.19	0.04	–	0.06	0.08	0.12	0.03	0.02	–	0.62	9.49
Sr	15.2	163	32.3	49.5	2025	476	148	–	0.89	9.30	23.9	13.2	34.8	236	29.2
Ba	–	7.20	36.4	304	2.76	3.46	1.14	–	0.86	0.41	1.60	1.29	1.28	158	203
Sc	10.1	27.6	50.8	50.3	31.9	28.7	22.3	41.8	30.5	21.6	8.32	28.3	28.8	15.7	1.62
V	115	409	209	340	329	325	393	45.7	20.1	25.1	187	372	474	264	176
Co	22.4	27.9	33.7	37.7	3.41	10.6	20.9	12.1	19.5	9.44	47.4	20.3	45.2	22.5	3.98
Zr	1.15	3.09	9.16	6.75	35.0	4.28	11.8	80.4	1.31	42.6	1.25	1.42	11.5	1.18	0.57
Y	3.54	0.55	39.0	29.2	61.9	7.95	2.38	132	140	95.9	16.3	–	1.92	0.66	0.69
Nb	0.11	29.9	4.81	6.29	23.2	4.47	0.71	6.60	0.26	0.43	0.03	1.53	0.05	0.18	0.39
Ta	0.03	5.29	0.33	0.57	4.18	0.32	0.17	0.25	0.14	–	–	0.45	–	–	0.04
Th	–	0.08	0.25	0.26	7.66	1.87	0.44	0.03	–	0.67	–	0.19	–	–	–
U	0.05	1.43	1.76	0.78	26.1	7.44	0.86	0.28	1.30	1.92	0.08	0.30	0.20	0.16	0.10
La	–	0.65	8.70	11.0	161	38.8	14.5	–	0.32	0.60	0.06	0.16	–	0.07	0.06
Ce	0.06	1.65	39.4	45.8	417	114	44.5	0.02	0.18	1.66	0.17	0.44	0.03	0.05	–
Pr	0.03	0.50	7.99	9.56	64.0	14.8	7.56	–	0.15	0.40	0.04	0.04	0.02	–	–
Nd	0.08	1.75	39.9	46.3	273	65.5	35.9	0.07	0.62	0.93	0.23	0.17	0.11	–	–
Sm	0.03	0.51	11.5	12.5	86.1	19.2	13.62	0.18	0.17	1.43	0.24	0.18	0.24	–	–
Eu	0.04	0.42	1.44	2.30	29.6	7.11	4.52	1.03	0.46	0.46	0.40	0.25	0.23	–	–
Gd	0.15	0.87	9.48	8.34	79.1	18.1	11.0	5.54	2.72	2.73	2.38	0.56	0.83	–	–
Tb	0.04	0.22	1.53	1.34	11.4	2.18	0.84	2.17	2.02	1.47	0.90	0.05	0.11	–	–
Dy	0.31	1.03	7.22	6.75	46.4	7.53	2.20	16.4	26.7	15.7	6.83	0.19	0.24	–	–
Ho	0.09	0.23	1.43	1.27	4.92	0.68	0.26	3.89	10.8	7.64	1.35	0.04	0.05	–	–
Er	0.23	0.82	3.70	2.69	6.42	0.98	0.40	11.9	32.0	37.8	3.68	0.10	0.09	–	–
Tm	0.03	0.13	0.51	0.36	0.49	0.11	0.04	1.85	3.88	7.46	0.54	0.02	–	–	–
Yb	0.17	0.84	2.90	2.02	2.80	0.44	0.25	13.2	23.0	59.7	3.40	0.10	0.21	–	–
Lu	0.03	0.16	0.45	0.21	0.37	0.04	0.05	2.08	2.54	11.1	0.55	0.02	0.08	–	–
ΣREE	1.29	9.78	136	150	1183	289	136	58.3	106	149	20.8	2.32	2.24	0.12	0.06
Eu/Eu*	1.82	1.93	0.42	0.69	1.10	1.17	1.13	3.16	2.07	0.71	1.62	2.41	1.58	–	–
La _N /Lu _N	–	0.43	2.04	5.54	46.1	103	30.7	–	0.01	0.01	0.01	0.85	–	–	–

1—high-P amphibolite; 2—foliated eclogite; 3—coronitic metagabbro; 4—granite (Verkhisetsk); c—core; r—rim.

5.2. Garnet

Garnet is almandine-rich in all rock types ($Alm_{0.56-0.69}$), with the highest pyrope values in eclogitic assemblages ($Py_{0.10-0.18}$). In the analysed high-P amphibolites, garnet shows no systematic compositional variations with almost flat core-rim profiles; whereas in garnet from eclogites, an increase in pyrope and a decrease in spessartine and grossular are observed towards the grain rims.

As observed in amphibole, garnet from eclogites shows significantly higher Sr contents than amphibolite garnet (Table 4, Fig. 3b). Garnet from foliated eclogites presents trace-element zoning, with Sr- and HREE- rich cores and rims enriched in Co, Y and MREE. In garnet from high-P amphibolites, slight trace-element zoning is also detected with cores enriched in V, Y, MREE and HREE. In coronitic garnets from metagabbros, core-rim trace-element variations cannot be detected owing to their small grain size, but the average from four grains shows minor variations for most trace elements (e.g. 27.8 ± 9.7 ppm Y, 33.7 ± 12 ppm Co). However, Sr contents are very varia-

ble (ca. 9.30 ± 15 ppm Sr), as observed in amphibole from foliated eclogites.

As in the case of amphiboles, garnet from foliated eclogites is richer in REE than garnet from high-P amphibolites. In most eclogitic garnets, chondrite-normalized REE-patterns are steeply positive from La to Dy–Ho and then decrease smoothly to Lu, with no Eu anomaly. Amphibolite garnet presents a chondrite-normalized REE pattern that is also very steep from La to Dy and then almost flat – or even slightly negative – to Lu; they have no Eu anomaly, near-zero LREE and less HREE than eclogitic garnets. Coronitic garnet shows chondritic REE patterns similar to those of amphibolitic garnet, with the same shape and REE abundance (see Fig. 5b).

5.3. Epidote-group minerals

Zoisite occurs in coronitic metagabbros with pistacite contents, Ps ($Ps = Fe^{3+}/(Fe^{3+} + Al-2)$), ranging from 0.11 to 0.33. In the other samples, epidote is progressively more Fe-rich showing Ps contents ranging from 0.50–0.68 in eclogites to 0.80–0.90 in high-P amphibolites.

Trace-element contents of epidote included in garnet could not be determined because of their small grain size. Matrix epidote in foliated eclogites and zoisite aggregates in coronitic metagabbros has abundant Li, Sr and V (> 50 ppm), moderate or high Ba, Sc, Co, Zr, Y, Th and U, and very low Rb and Cs (Fig. 3c).

Epidote shows the largest Sr (and LREE) variations at single grain scale. Microprobe analyses of LREE and Sr in an epidote grain from a foliated eclogite (Table 5) show strong compositional zoning with Sr ranging from > 4000 to ~300 ppm, and La and Ce from ~2000 and ~6000 ppm, respectively, to concentrations close to detection limit. BSE images (Fig. 6) show that the high Sr and LREE concentrations occur in very small (a few micrometers) irregular patches related to rutile inclusions.

Chondrite-normalized REE patterns are almost flat from La to Gd and then decrease smoothly from Gd to Lu, with $Gd_N/Yb_N = 22.8$ – 35.8 showing high LREE/HREE fractionation ($La_N/Lu_N = 45$ to 100) (Fig. 5c). The Eu anomaly is moderately positive ($Eu/Eu^* = 1.10$ – 1.17), as in epidote from other low-T metamorphic settings

(e.g. Nystrom, 1984; Tribuzio et al., 1996). These compositional features contrast with epidote from subduction-related plutonic acid rocks (e.g. granodiorites and granites from Verkhisetsk, Urals, Russia; Bea, 1996), which presents strong positive Eu anomalies and lower LREE/HREE ratios (e.g. $La_N/Lu_N = 30$ for epidotes from the Verkhisetsk granite, F. Bea, pers. comm.).

5.4. Clinopyroxene

Clinopyroxene has omphacite composition with minor acmite substitution and negligible Al^{IV} contents. It contains high Li and V (> 100 ppm), moderate to low Sr, Ba, Co, Y and Zr (~1–50 ppm), and very low Rb, Cs, Nb, Ta, Th and U (Fig. 3d). REE contents are also low ($\Sigma REE = 2.32$ – 1.23). In both foliated and coronitic metagabbros, clinopyroxene is relatively homogeneous at sample scale (e.g. $\sim 350 \pm 17$ ppm V, $\sim 30 \pm 7$ ppm Sc, $\sim 0.16 \pm 0.01$ ppm La).

In clinopyroxene from foliated eclogites, chondrite-normalized REE patterns decrease from La to Nd, then increase towards Eu, showing a small positive Eu anomaly ($Eu/Eu^* = 0.98$ – 2.40), and decrease towards Dy, becoming almost flat from Dy to Lu (Fig. 5d). In coronitic metagabbros, clinopyroxene shows S-shaped chondrite-normalized REE patterns, which increase from La to Eu, decrease to Tm, and then increase again to Lu.

5.5. White mica

Na-mica is very close to the ideal paragonite composition, while K-mica exhibits more complex compositions with some phengitic substitution ($Si = 3.23$ – 3.29 apfu) and Na contents of up to 0.14 apfu.

In paragonite from eclogites and high-P amphibolites, Li, Rb, Ba, Sr and V are high, Cs, Sc, Co,

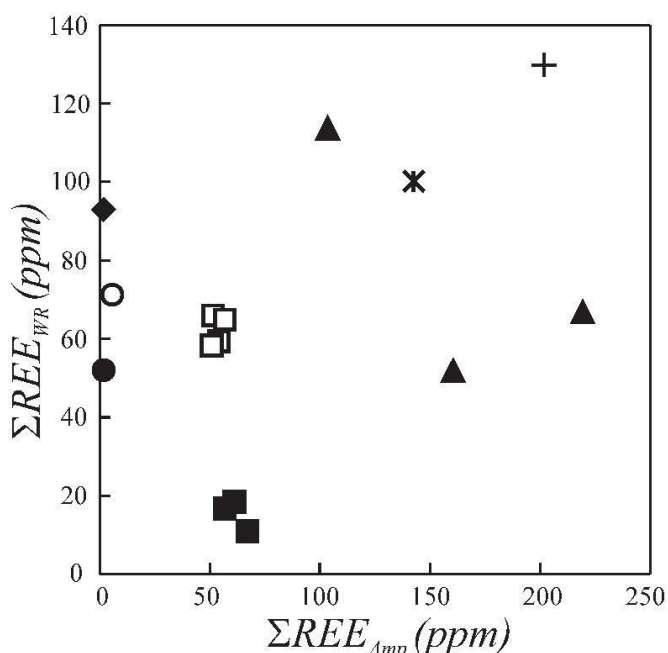


Fig. 4 ΣREE_{Amp} vs. ΣREE_{WR} in high-P amphibolites and eclogites from the Nevado-Filábride complex compared with values for other rock types. Filled circle: high-P amphibolite (paragonite-rich type); filled diamond: high-P amphibolite (phengite-rich type); cross: Fe-gabbro from Liguria (Tribuzio et al., 1996); filled square: spinel lherzolite from S Baikal (Ionov et al., 1993) and amphibole-rich peridotite from E Pyrenees (Bodinier et al., 1988); open square: andesite from Colima Volcanic complex (Luhr and Carmichael, 1980); filled triangle: dacite from S Kyushu (Nagasawa and Schnetzler, 1971); asterisk: granite from Verkhisetsk (Bea, unpublished).

Table 5 Microprobe analyses of major elements, Sr, La and Ce in epidote (foliated eclogites)¹.

	1	2	3
(wt%)			
SiO ₂	36.7	37.6	37.9
Al ₂ O ₃	24.5	23.9	24.1
Fe ₂ O ₃	9.98	11.3	10.6
MnO	0.17	0.09	0.06
CaO	22.0	23.3	23.9
Total	93.4	96.2	96.6
(ppm)			
Sr	4378	1691	298
La	2089	bdl	bdl
Ce	5870	298	bdl

¹ see BSE image in Fig. 6 for analysis location. bdl—below detection limit.

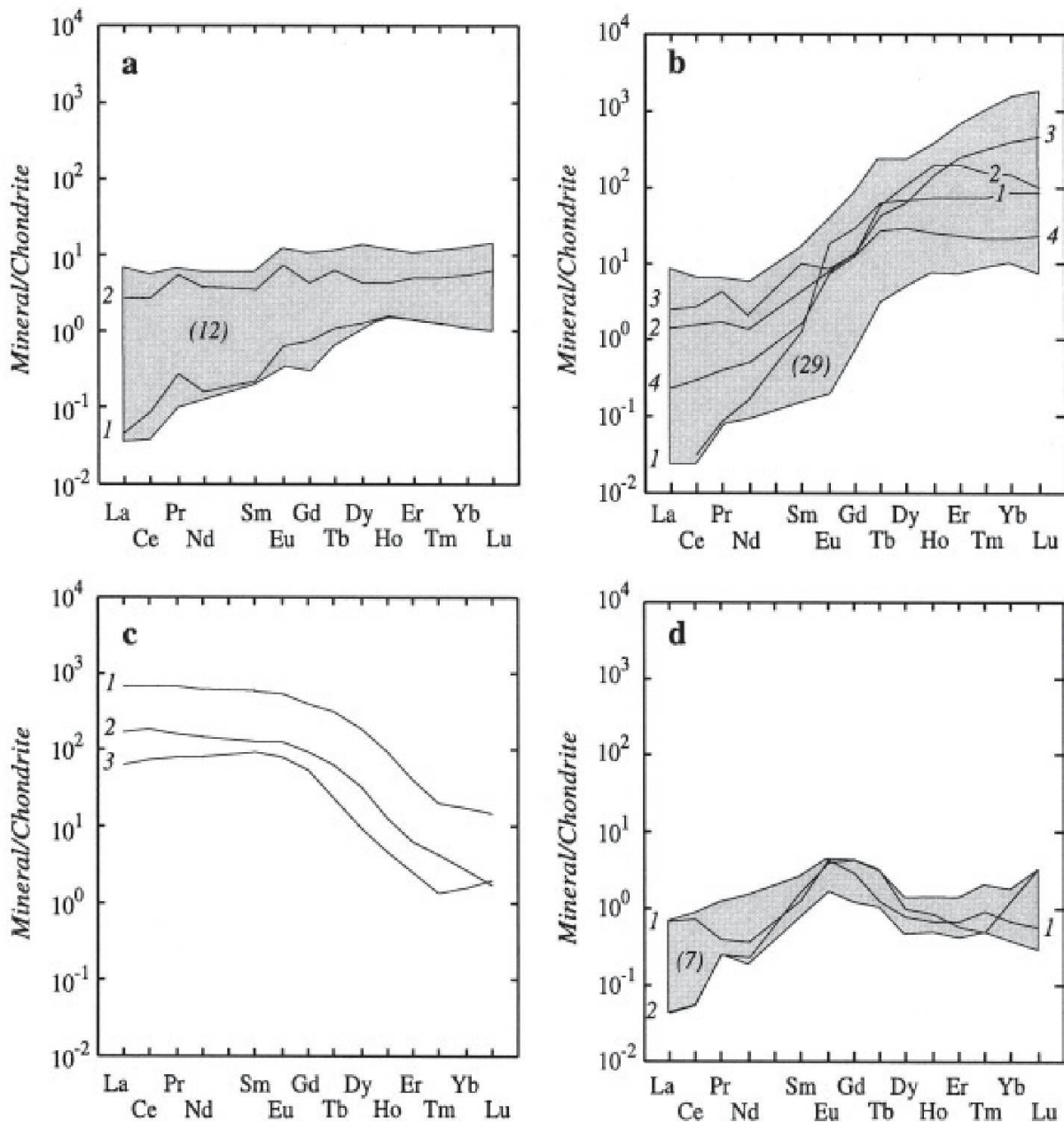


Fig. 5 Chondrite-normalized REE patterns of amphibole, garnet, epidote and pyroxene from high-P amphibolites and eclogites from the Nevado-Filábride complex. (a) Amphibole: 1, high-P amphibolite; 2, foliated eclogite. (b) Garnet: 1, high-P amphibolite; 2 (rim) and 3 (core), foliated eclogite; 4, coronitic metagabbro. (c) Epidote: 1-2, foliated eclogite; 3, coronitic metagabbro. (d) Clinopyroxene: 1, foliated eclogite; 2, coronitic metagabbro. See Table 4 for trace-element mineral analyses. Shaded areas represent fields occupied by analysed grains; the number of analyses is given in brackets. Chondrite values are from Anders and Ebihara (1982).

Zr and Y are moderate or low, and Nb, Ta, Th and U are very low, while phengite is richer in Rb and Cs (Fig. 3e). In both types of micas, REE contents are very low ($\Sigma\text{REE} = 4.75\text{--}0.06$ ppm), in most cases below detection limits, which is a common feature of micas (Bea, 1996).

6. Discussion

Sr and LREE are highly variable in the eclogite-facies minerals, which contrasts with the minor trace-element variations observed in the mineral phases from high-P amphibolites.

However, in spite of the strong trace-element zoning in eclogitic minerals, major-element data reported by Molina and Poli (1998) for amphibole and omphacite from the rock matrix of foliated eclogites show minor variations. In addition, Fe/Mg partition coefficients between amphibole, omphacite and garnet suggest the attainment of equilibrium of grain rims (Molina and Poli, 1998). These relationships provide evidence for the higher sensitivity of trace elements to kinetic processes as suggested by Hickmott et al., (1987) and Hickmott and Shimizu (1990).

Trace-element zoning in garnet porphyroblasts may be partly caused by trace-element frac-

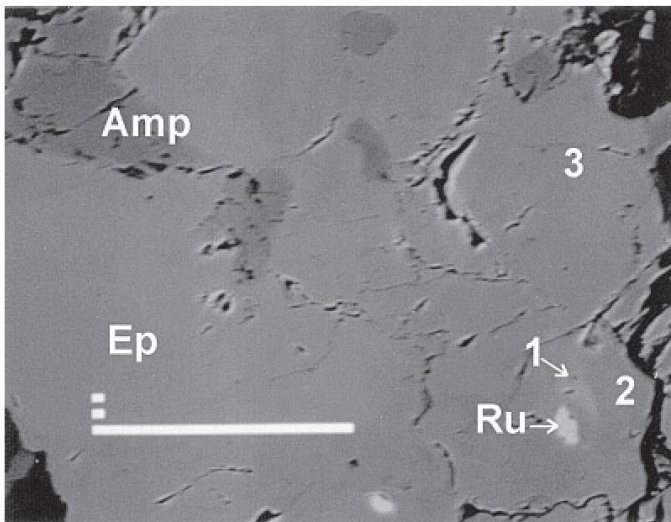


Fig. 6 BSE image of epidote in foliated eclogite. Bright area close to rutile inclusion is very rich in Sr and LREE. Numbers refer to microprobe analyses in Table 5. Scale bar is 100 μm .

tiation during garnet growth (i.e. growth zoning, Hollister, 1966). However, this mechanism cannot explain the abrupt Sr and LREE variations observed in epidote. Zoisite and epidote with Sr and LREE zonation like those from the Nevado-Filábride eclogites have been reported in numerous high-*P* terrains: Norwegian Caledonides (Brastad, 1985), North Cascades (Sorensen and Grossman, 1993), Catalina Schist (California) (Sorensen and Grossman, 1993) and Su-Lu province (eastern China) (Nagasaki and Enami, 1998). Two mechanisms have been proposed to explain the Sr and/or LREE zonation: (1) breakdown of Sr-REE-rich accessory minerals during mineral growth with local trace-element transport (at millimetre scales), i.e. internal metasomatism (Hickmott et al., 1987); and (2) introduction of Sr and REE into the rock by externally-derived fluids, which implies trace-element transport of, at least, decimetre scales, i.e. external metasomatism (Hickmott et al., 1987). Nagasaki and Enami (1998) suggested local variations in the Sr contents of the protoliths to account for zoned Sr-rich zoisite and epidote in the ultrahigh-*P* rocks from the Su-Lu province. By contrast, Brastad (1985) invoked the infiltration of Sr-rich fluids into the rock to explain anomalous Sr concentrations in Ca-rich minerals from Norwegian eclogites. In agreement with external metasomatism-based mechanisms, Sorensen and Grossman (1993) attribute zoned REE-rich epidotes in North Cascades and in Catalina Schist to subduction-related fluid-rock interaction processes.

In the epidotes from Nevado-Filábride eclogites, the occurrence of rutile in close connection to the Sr-LREE-rich domains suggest that abrupt changes may have been caused by the breakdown

of titanite during the eclogite-facies metamorphism. Titanite can contain significantly higher Sr and LREE contents than rutile and, hence, relatively large amounts of these trace elements may be released from titanite during metamorphism leading to local domains enriched in Sr and LREE if mass transport through the rock matrix was limited. This mechanism is likely since titanite had probably formed prior to the eclogite-facies metamorphism (e.g. Gómez-Pugnaire and Fernández-Soler, 1987; Molina, 1995).

Limited mass transport across the rock matrix during eclogite-facies metamorphism has been also argued to explain the preservation of fine-scale trace-element heterogeneities in Alpine eclogites (Getty and Selverstone, 1994). This contrasts with the epidote segregation observed in the high-*P* amphibolites. Although segregation prior to the high-*P* metamorphism cannot be disregarded, the systematic presence of epidote grains included in garnet supports the segregation of epidote during the growth of the garnet porphyroblasts and, hence, during high-*P* metamorphism. The segregation of epidote requires dissolution of epidote, transport of its chemical components on, at least, centimetre-to-metre-scales, and nucleation and growth of the new epidote grains. Given the relatively low temperatures of metamorphism, volume diffusion is precluded and mass transport should be produced by grain-boundary diffusion enhanced by a fast intergranular medium – either a volatile-rich fluid phase or a volatile-rich surface film adsorbed on crystal surfaces (e.g. Fisher, 1973). The depletion in LREE detected in the mineral phases from high-*P* amphibolites and in their bulk composition suggest that REE could also be transported towards epidote segregates by the intergranular medium. Therefore, this leads to a redistribution of REE and Sr in the high-*P* amphibolites controlled by the kinetic of nucleation and growth of epidote grains.

The preservation of trace-element zoning in foliated eclogites shows that deformation was not an efficient mechanism for eliminating compositional heterogeneities even in minerals defining the matrix foliation. Therefore, the different trace-element behaviour reported in eclogites and in high-*P* amphibolites can be related to different scales of fluid circulation during the high-*P* metamorphism.

Zoisite and epidote may play a key role in the transport of REE to great depth at convergent margins, as result of their stability to ultrahigh-*P* conditions (Poli and Schmidt, 1995, 1998). Therefore, experimental determinations of epidote/fluid partition coefficients for Sr and LREE are essential to assess the transfer of these trace ele-

ments to the mantle wedge at convergent margins. However, if their distribution in high-P minerals is heterogeneous as indicated by epidote from the Nevado-Filábride eclogites, disequilibrium models for trace-element releasing and transport, including the kinetics of nucleation and growth of epidote-group minerals and other Sr-LREE-rich minerals, which may be stable at eclogite-facies conditions (e.g. allanite and apatite), must be considered to obtain effective rock/fluid partition coefficients for LREE and Sr at high-P conditions.

7. Conclusions

Trace-element abundances of major-silicate phases from high-P mafic rocks from the Nevado-Filábride complex show that Rb, Cs and Ba are concentrated in mica, Y and HREE in garnet, and Sr and LREE in epidote group minerals, whereas amphibole and clinopyroxene show very low REE contents as is commonly observed in high-P mafic rocks.

In spite of attainment of major-element equilibrium partitioning in foliated eclogites, large scattering occurs in the distribution of Sr and LREE. This may suggest limited capacity of the intergranular medium in eclogites to eliminate heterogeneities in Sr and LREE contents through the rock. The high-P amphibolites have remarkably different trace-element behaviour with only minor scattering. This difference may suggest that fluids strongly control trace-element mobility and promote attainment of equilibrium in the latter.

The likelihood of heterogeneous distribution of LREE and Sr prior to the eclogite-facies metamorphism owing to the existence of pre-eclogitic Sr-LREE-rich minerals such as titanite, allanite or apatite evidences that the recycling of these trace elements at convergent margins may be controlled by disequilibrium fluid-rock interaction processes.

Acknowledgements

The authors are very grateful to F. Bea and M.T. Gómez-Pugnaire, who encouraged us to study trace-element residence in high-P mafic rocks. We thank H. Austrheim, F. Bea, S. Poli, E. Rampone, J.H. Scarrow and M. Tiepolo for their constructive comments. We also thank H. Austrheim and M. Erambert for help with the microprobe work at the Mineralogisk-Geologisk Museum of Oslo (Norway). The help of C. Laurin and J.H. Scarrow in improving the English is also gratefully acknowledged. Helpful comments of two anonymous reviews resulted in improvements to the manuscript. The editorial handling of M. Engi is also acknowledged. Thanks are given to Perkin Elmer Corp., which kindly permitted the use of its LA-ICP-MS laboratory at Überlingen (Germany). This work has been financed by the Spanish DGICYT projects AMB93-0535, AMB94-1420, PB95-1266 and

BTE2002-04618-CO2-01 and by grants FPI and FPI en el extranjero of the Spanish MEC and grant of the European Commission (TMR-URO Programme, contract ERBFMRXCT960009).

References

- Anders, E. and Ebihara, M. (1982): Solar-system abundances of the elements. *Geochim. Cosmochim. Acta* **46**, 2363–2380.
- Austrheim, H., Erambert, M. and Engvik, A.K. (1997): Processing of crust in the root of the Caledonian continental collision zone: the role of eclogitization. *Tectonophysics* **273**, 129–153.
- Ayers, J.C., Dittmer, S.K. and Layne, G.D. (1997): Partitioning of elements between peridotite and H₂O at 2.0–3.0 Gpa and 900–1000 °C, and application to models of subduction zone processes. *Earth Planet. Sci. Lett.* **150**, 381–398.
- Bea, F. (1996): Residence of REE, Y, Th and U in granites and crustal protoliths; Implications for the chemistry of crustal melts. *J. Petrol.* **37**, 521–552.
- Bea, F., Montero, P., Garuti, G. and Zacharinni, F. (1998): Pressure-dependence of rare earth element distribution in amphibolite- and granulite-grade garnets. A LA-ICP-MS study. *Geostandards Newsletters* **21**, 253–270.
- Bea, F., Montero, P., Stroh, A. and Basner, J. (1996): Microanalysis of minerals by an Eximer UV-LA-ICP-MS system. *Chem. Geol.* **133**, 145–156.
- Bea, F., Pereira, M.D. and Stroh, A. (1994): Mineral/leucosome trace-element partitioning in a peraluminous migmatite (a laser ablation ICP-MS study). *Chem. Geol.* **117**, 291–312.
- Bebout, G. and Barton, M.D. (1993): Metasomatism during subduction: products and possible paths in the Catalina Schist, California. *Chem. Geol.* **108**, 61–92.
- Bodinier, J.L., Dupuy, C. and Dostal, J. (1988): Geochemistry and petrogenesis of Eastern Pyrenean peridotites. *Geochim. Cosmochim. Acta* **52**, 2893–2907.
- Brenan, J.M., Shaw, H.F. and Ryerson, F. (1995a): Experimental evidence for the origin of lead enrichment in convergent-margin magmas. *Nature* **378**, 54–56.
- Brenan, J.M., Shaw, H.F., Ryerson, F.J. and Phinney, D.L. (1995b): Mineral-aqueous fluid partitioning of trace elements at 900 °C and 2.0 GPa: constraints on the trace element chemistry of mantle and deep crustal fluids. *Geochim. Cosmochim. Acta* **59**, 3331–3350.
- Brastad, K. (1985): Sr metasomatism, and partition of Sr between mineral phases of a meta-eclogite from Bjorkedal, West Norway. *Tsch. Mineral. Petrogr. Mitt.* **34**, 87–103.
- Elliot, T., Plank, T., Zindler, A., White, W. and Bourdorn, B. (1997): Element transport from slab to volcanic front at the Mariana Arc. *J. Geophys. Res.* **102**, 14991–15019.
- Fisher, G.W. (1973): Non-equilibrium thermodynamics as a model for diffusion-controlled metamorphic processes. *Am. J. Sci.* **273**, 897–924.
- García-Dueñas, V., Balanya, J.C. and Martínez-Martínez, J.M. (1992): Miocene extensional detachments in the outcropping basement of the northern Alborán Basin (Betics) and their tectonic implications. *Geo. Marine Lett.* **12**, 88–95.
- Getty, S.R. and Selverstone, J. (1994): Stable isotopic and trace-element evidence for restricted fluid migration in 2 Gpa eclogite. *J. Metamorphic Geol.* **12**, 747–760.
- Gómez-Pugnaire, M.T. and Fernández-Soler, J.M. (1987): High-pressure metamorphism in metabasites from the Betic Cordilleras (SE Spain) and its evolution during the Alpine orogeny. *Contrib. Mineral. Petrol.* **95**, 231–244.

- Gómez-Pugnaire, M.T. and Muñoz, M. (1991): Al-rich xenoliths in the Nevado-Filábride metabasites: evidence for a continental magmatism in the Betic Cordilleras (SE Spain). *Eur. J. Mineral.* **3**, 193–198.
- Gómez-Pugnaire, M.T., Ulmer, P. and López-Sánchez-Vizcaíno, V. (2000): Petrogenesis of the mafic igneous rocks of the Betic Cordilleras: A field, petrological and geochemical study. *Contrib. Mineral. Petrol.* **139**, 436–457.
- Hermann, J. (2002): Allanite: thorium and light rare earth element carrier in subducted crust. *Chem. Geol.* **192**, 289–306.
- Hickmott., D.D. and Shimizu, N. (1990): Trace-element zoning in garnet from the Kwoiek area, British Columbia: disequilibrium partitioning during garnet growth? *Contrib. Mineral. Petrol.* **104**, 619–630.
- Hickmott., D.D., Shimizu, N., Spear, F.S. and Selverstone, J. (1987): Trace-element zoning in a metamorphic garnet. *Geology* **15**, 573–576.
- Hollister, L.S. (1966): Garnet zoning: An interpretation based on the Rayleigh fractionation model. *Science* **154**, 1647–1650.
- Ionov, D.A., Griffin, W.L. and O'Reilly, S.Y. (1997): Volatile-bearing minerals and lithophile trace elements in the upper mantle. *Chem. Geol.* **141**, 153–184.
- Ionov, D.A., Kram, U. and Stosch, H.G. (1993): Evolution of the upper mantle beneath the southern Baikal rift zone: Sr–Nd isotope study of xenoliths from the Bartoy volcanoes. *Contrib. Mineral. Petrol.* **111**, 235–247.
- Jabaloy, A., Galindo-Zaldívar, J. and González-Lodeiro, F. (1993): The Alpujarride–Nevado-Filábride extensional shear zone, Betic Cordillera, SE Spain. *J. Struct. Geol.* **15**, 555–569.
- Keppler, H. (1996): Constraints from partitioning experiments on the composition of subduction-zone fluids. *Nature* **380**, 237–240.
- López-Sánchez-Vizcaíno, V., Connolly, J.A.D. and Gómez-Pugnaire, M.T. (1997): Metamorphism and phase relations in carbonate rocks from the Nevado-Filábride Complex (Cordilleras Béticas, Spain): application of the Ttn + Rt + Cal + Qtz + Gr buffer. *Contrib. Mineral. Petrol.* **126**, 292–302.
- Luhr, J.F. and Carmichael, I.S.E. (1980): The Colima Volcanic Complex, Mexico. I Post-caldera andesites from Volcán Colima. *Contrib. Mineral. Petrol.* **71**, 342–372.
- Messiga, B., Tribuzio, R., Bottazzi, P. and Ottolini, L. (1995): An ion microprobe study on trace-element composition of pyroxenes from blueschist and eclogitized Fe-Ti-gabbros, Ligurian Alps, northwestern Italy: some petrologic considerations. *Geochim. Cosmochim. Acta* **59**, 59–75.
- Molina, J.F. (1995): Geochemical and petrological evolution of the mafic schists from the Nevado-Filábride complex, Betic Cordilleras, Spain. Unpub. PhD. Thesis, University of Granada (Spain), 250 pp. (in Spanish)
- Molina, J.F. and Poli, S. (1998): Singular equilibria in paragonite blueschists, amphibolites and eclogites. *J. Petrol.* **39**, 1325–1346.
- Molina, J.F. and Poli, S. (2000): Carbonate stability and fluid composition in subducted oceanic crust: an experimental study on H₂O–CO₂-bearing basalts. *Earth Planet. Sci. Lett.* **176**, 295–310.
- Nagasaki, A. and Enami, M. (1998): Sr-bearing zoisite and epidote in ultra-high pressure (UHP) metamorphic rocks from the Su-Lu province, eastern China: an important Sr reservoir under UHP conditions. *Am. Mineral.* **38**, 240–247.
- Nagasawa, H. and Schnetzler, C.C. (1971): Partitioning of rare earth, alkali and alkaline earth elements between phenocrysts and acidic igneous magma. *Geochim. Cosmochim. Acta* **35**, 953–968.
- Nystrom, J.O. (1984): Rare earth element mobility in vesicular lava during low-grade metamorphism. *Contrib. Mineral. Petrol.* **88**, 328–331.
- Poli, S. (1993): The amphibole-eclogite transformation, an experimental study on basalt. *Am. J. Sci.* **293**, 1061–1107.
- Poli, S. and Schmidt, M.W. (1995): H₂O transport and release in subduction zones: experimental constraints on basaltic and andesitic systems. *J. Geophys. Res.* **100**, 22299–22314.
- Poli, S. and Schmidt, M.W. (1998): The high-pressure of zoisite and phase relationships of zoisite-bearing assemblages. *Contrib. Mineral. Petrol.* **130**, 162–175.
- Poli, S. and Schmidt, M.W. (2002): Petrology of subducted slabs. *Annu. Rev. Earth Planet. Sci.* **30**, 207–235.
- Rampone, E., Piccardo, G.B., Vannucci, R., Bottazzi, P. and Ottolini, L. (1993): Subsolvus reactions monitored by trace-element partitioning: The spinel-to plagioclase-facies transition in mantle peridotites. *Contrib. Mineral. Petrol.* **115**, 1–17.
- Ryan, J.G., Leeman, W.L., Morris, J.D. and Langmuir, C.H. (1996): The boron systematics of intraplate lavas: implications for crust and mantle evolution. *Geochim. Cosmochim. Acta* **60**, 415–422.
- Saunders, A.D., Tarney, J. and Weaver, S.D. (1980): Transverse geochemical variations across the Antarctic peninsula: implications for the genesis of calc-alkaline magmas. *Earth Planet. Sci. Lett.* **46**, 344–360.
- Scambelluri, M. and Philippot, P. (2001): Deep fluids in subduction zones. *Lithos* **55**, 213–227.
- Schmidt, M.W. and Poli, S. (1998): Experimentally based water budgets for dehydrating slabs and consequences for arc magma generation. *Earth Planet. Sci. Lett.* **163**, 361–379.
- Selverstone, J., Franz, G., Thomas, S. and Getty, S. (1992): Fluid variability in 2 GPa eclogites as indicator of fluid behaviour during subduction. *Contrib. Mineral. Petrol.* **112**, 341–357.
- Sørensen, S.S. and Grossman, J.N. (1989): Enrichment of trace elements in garnet amphibolites from Catalina Schist, southern California. *Geochim. Cosmochim. Acta* **53**, 3155–3177.
- Sørensen, S.S. and Grossman, J.N. (1993): Accessory minerals and subduction zone metasomatism: a geochemical comparison of two mélanges (Washington and California, U.S.A.). *Chem. Geol.* **110**, 269–297.
- Tatsumi, Y. and Eggins, S. (1993): Subduction zone magmatism. *Frontiers in Earth Science*. Blackwell Science, 211 pp.
- Tribuzio, R., Messiga, B., Vannucci, R. and Bottazzi, P. (1996): Rare earth element redistribution during high-pressure-low temperature metamorphism in ophiolitic Fe-gabbros (Liguria, northwestern Italy): Implications for light REE mobility in subduction zones. *Geology* **24**, 711–714.
- Zack, T., Rivers, T. and Foley, S.F. (2001): Cs–Rb–Ba systematics in phengite and amphibole: an assessment of fluid mobility at 2.0 GPa in eclogites from Trescolmen, Central Alps. *Contrib. Mineral. Petrol.* **140**, 651–669.
- Zanetti, A., Vannucci, R., Bottazzi, P., Oberti, R. and Ottolini, L. (1996): Infiltration metasomatism at Lherz as monitored by systematic ion-microprobe investigations close to a hornblendite vein. *Chem. Geol.* **134**, 113–133.

Received 13 December 2001

Accepted in revised form 9 June 2003

Editorial handling: M. Engi